

Active Power Control Strategies for Inverter-Based Distributed Power Generation Adapted to Grid-Fault Ride-Through Requirements

Fei Wang, Jorge L. Duarte, and Marcel A. M. Hendrix
Department of Electrical Engineering
Eindhoven University of Technology
5600 MB Eindhoven, The Netherlands
Phone: +31 40 247 3566
Fax: +31 40 243 4364
Email: f.wang@tue.nl
URL: <http://w3.ele.tue.nl/epe>

Keywords

<<Power control>>, <<Power quality>>, <<Renewable energy systems>>, <<Voltage source inverters>>

Abstract

Distributed power generation is expected to deliver power into the grid without interruption during voltage dips. To improve system ride-through capabilities, a generalized active power control strategy is proposed for grid-interfacing inverters. Specifically, a current reference generation strategy based on symmetric-sequence components of unbalanced three-phase three-wire or four-wire systems is derived. It is shown that a single adjustable parameter can smoothly change the relative amplitudes of oscillating active and reactive power. This steering possibility enables grid-side inverters to optimally meet different requirements of coming standards. Simulations and experiments are carried out to validate the proposed strategy.

Introduction

Voltage dips appear in balanced or unbalanced situations, where balanced dips are infrequent. When dips remain for prolonged time periods, power electronics based distributed generation (DG) systems normally disconnects from the grid. However, large scale inverter-based grid-connected DG, especially wind farms, are required by utility grid codes [1] to tolerate voltage dips without interruption. The reason is to maintain active or reactive power delivery for supporting the grid. To achieve this two aspects should be noticed, that are fast dynamic response at the occurrence of voltage dips or fault recovery, and an optimal selection of reference current during the period of voltage dips. This paper focuses on grid-side inverters and their current reference generation. During unbalanced voltage dips, current reference generation should take into account low-order dc voltage variations in the DC bus, symmetry of currents, and maximum power tracking. [2]-[4].

Many inverter-based DG systems deliver power to the grid by controlling injected currents. Assuming controllers are fast enough at the moment of voltage dips, then the only difference before and after a grid fault is a change in demanded current. Different methods can be used to construct the desired current references. Due to asymmetry of phase voltages, methods based only on instantaneous power theory [5] will generate distorted and unbalanced reference currents that are not preferred from the power quality point of view. Alternatively, symmetric-sequence components based strategies can easily obtain sinusoidal reference currents. As presented in [6], several current control strategies were investigated based on different application schemes of positive and negative sequences, showing the flexibility of active power control.

This paper intends to derive a generalized strategy for active power control based on symmetric-sequence components. Through a continuously adjustable parameter, it is possible to change the relative ampli-

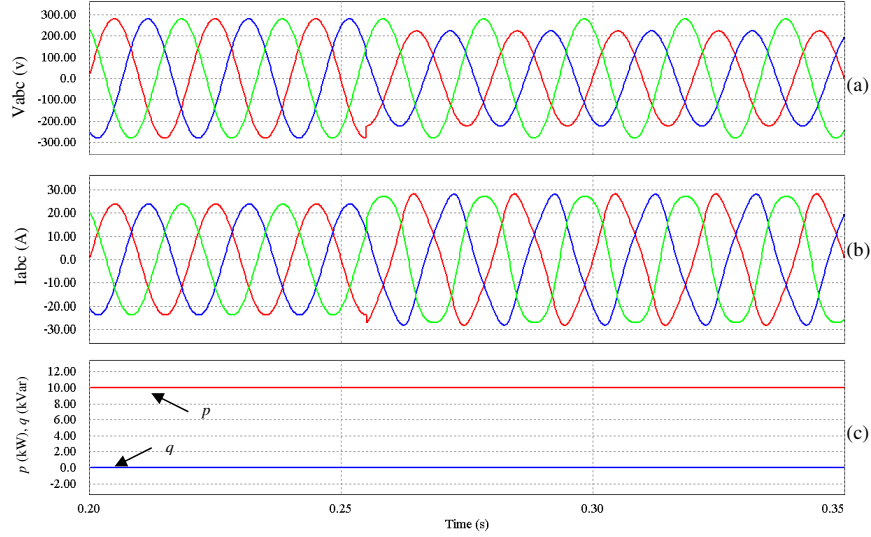


Fig. 1: Simulation results obtained from instantaneous power theory with $P=10\text{kW}$, $Q=0$, where voltages of phase A and B dip to 80% at $t=0.25\text{s}$, (a) phase voltages, (b) injected currents, (c) instantaneous p , q .

tudes of oscillating active and reactive power smoothly, and to eliminate the second-order active or reactive power ripple at the two extremes of the coefficient range. In other words, current can be optimized with respect to voltage dips and some practical constraints. An additional problem with voltage dips is that the zero sequence voltage appears on the user terminals through star-star grounded distribution transformers. Hardly any work has been done to analyze active power control of a four-wire system by taking into account zero sequence components of unbalanced voltages. To this purpose, the paper also investigates the contribution of zero-sequence components to current reference generation. Finally, simulation and experiments are carried out to verify the proposed methods.

Review of instantaneous power theory

Instantaneous active power and reactive power calculated in a-b-c frame are defined [5] by, respectively,

$$p = \mathbf{v} \cdot \mathbf{i} = v_a i_a + v_b i_b + v_c i_c \quad (1)$$

$$q = \mathbf{v}_\perp \cdot \mathbf{i} = \frac{1}{\sqrt{3}} [(v_a - v_b) i_c + (v_b - v_c) i_a + (v_c - v_a) i_b] \quad \text{with} \quad \mathbf{v}_\perp = \frac{1}{\sqrt{3}} \begin{bmatrix} 0 & 1 & -1 \\ -1 & 0 & 1 \\ 1 & -1 & 0 \end{bmatrix} \mathbf{v}, \quad (2)$$

where $\mathbf{v} = [v_a \ v_b \ v_c]^T$, $\mathbf{i} = [i_a \ i_b \ i_c]^T$, bold symbols represent vectors, and the operator “ \cdot ” denotes the dot product of vectors. To deliver a given constant active power (P) and zero reactive power, the corresponding currents can be calculated based on instantaneous power theory. The derived currents, denoted by \mathbf{i}_p , are expressed by

$$\mathbf{i}_p = \frac{P}{\|\mathbf{v}\|^2} \mathbf{v}, \quad (3)$$

where $\|\mathbf{v}\|^2 = \mathbf{v} \cdot \mathbf{v} = v_a^2 + v_b^2 + v_c^2$, operator “ $\|\cdot\|$ ” means the norm of a vector, and subscript “ p ” represents active power control related. Since \mathbf{i}_p is in phase with \mathbf{v} , the resulting instantaneous reactive power q in (2) equals zero. Because $\|\mathbf{v}\|$ is constant when the voltages are balanced, derived currents are balanced and sinusoidal waveforms. However, when the voltage \mathbf{v} becomes unbalanced, $\|\mathbf{v}\|$ is not a constant any more, but varies with twice the fundamental frequency. Consequently, reference currents \mathbf{i}_p becomes distorted and unbalanced, as illustrated in Fig. 1.

Although with the method of instantaneous power control, constant active and reactive power can be achieved at the cost of current distortion, it may not be acceptable to inject low quality currents into the grid even during voltage dips. Moreover, the current distortion can become worse in other unbalanced

dip conditions and cause harmonics propagation through the grid. It is conceivable to employ only fundamental quantities for sinusoidal current generation. Therefore, an instantaneous power theory based on symmetric-sequence components is derived in the following.

Phasorial notation is a proven and convenient way to describe sinusoidal quantities. For instance, where harmonics are neglectable, quantities in a-b-c frame can be expressed by

$$\mathbf{v} = \begin{bmatrix} v_a \\ v_b \\ v_c \end{bmatrix} = \Re \left(e^{j\omega t} \begin{bmatrix} \underline{V}_a \\ \underline{V}_b \\ \underline{V}_c \end{bmatrix} \right), \quad (4)$$

where phasors are denoted with a bar subscript, and $\Re(\cdot)$ represents the real part of a complex number. Applying symmetric-component transformation to voltage phasors yields symmetric-component phasors as

$$\begin{bmatrix} \underline{V}^0 \\ \underline{V}^+ \\ \underline{V}^- \end{bmatrix} = \frac{1}{3} \begin{bmatrix} 1 & 1 & 1 \\ 1 & a & a^2 \\ 1 & a^2 & a \end{bmatrix} \begin{bmatrix} \underline{V}_a \\ \underline{V}_b \\ \underline{V}_c \end{bmatrix}, \text{ with } a = e^{j\frac{2\pi}{3}}, \quad (5)$$

where subscripts "+", "-", and "0" denote positive, negative, and zero sequences, respectively. The inverse transformation of (5) is found to be

$$\begin{bmatrix} \underline{V}_a \\ \underline{V}_b \\ \underline{V}_c \end{bmatrix} = \begin{bmatrix} 1 & 1 & 1 \\ 1 & a^2 & a \\ 1 & a & a^2 \end{bmatrix} \begin{bmatrix} \underline{V}^0 \\ \underline{V}^+ \\ \underline{V}^- \end{bmatrix}. \quad (6)$$

Correspondingly, instantaneous values can be derived from the symmetric-component phasors given by (6). Otherwise stated, the following expressions for the a-b-c voltage are applicable:

$$\mathbf{v} = \mathbf{v}^+ + \mathbf{v}^- + \mathbf{v}^0 \quad (7)$$

$$\text{with } \mathbf{v}^+ = \begin{bmatrix} v_a^+ \\ v_b^+ \\ v_c^+ \end{bmatrix} = \Re \left(\underline{V}^+ e^{j\omega t} \begin{bmatrix} 1 \\ a^2 \\ a \end{bmatrix} \right), \mathbf{v}^- = \begin{bmatrix} v_a^- \\ v_b^- \\ v_c^- \end{bmatrix} = \Re \left(\underline{V}^- e^{j\omega t} \begin{bmatrix} 1 \\ a \\ a^2 \end{bmatrix} \right), \text{ and}$$

$$\mathbf{v}^0 = \begin{bmatrix} v_a^0 \\ v_b^0 \\ v_c^0 \end{bmatrix} = \Re \left(\underline{V}^0 e^{j\omega t} \begin{bmatrix} 1 \\ 1 \\ 1 \end{bmatrix} \right).$$

Similarly, current quantities may also be represented in terms of symmetric sequences, i.e.

$$\mathbf{i} = \mathbf{i}^+ + \mathbf{i}^- + \mathbf{i}^0 \quad (8)$$

where $\mathbf{i}^{+, -, 0} = \begin{bmatrix} i_a^{+, -, 0} & i_b^{+, -, 0} & i_c^{+, -, 0} \end{bmatrix}^T$. As a result, the calculation of instantaneous power in (1) and (2) can be rewritten as

$$p = \mathbf{v} \cdot \mathbf{i} = (\mathbf{v}^+ + \mathbf{v}^- + \mathbf{v}^0) \cdot (\mathbf{i}^+ + \mathbf{i}^- + \mathbf{i}^0), \quad (9)$$

$$q = \mathbf{v}_\perp \cdot \mathbf{i} = (\mathbf{v}_\perp^+ + \mathbf{v}_\perp^- + \mathbf{v}_\perp^0) \cdot (\mathbf{i}^+ + \mathbf{i}^- + \mathbf{i}^0). \quad (10)$$

Based on this symmetric-sequence-based power definition, a comprehensive investigation on how to generate sinusoidal current references for the current control of inverter-based DG systems is presented in the next sections. Note that calculating instantaneous power and current references is carried out in terms of vectors. Hence, these calculations can also be used in other reference frames, simply by substituting the vectors in a-b-c frames with vectors in other frames, for example, the stationary $\alpha - \beta - \gamma$ reference frame.

Current reference generation for active power control

In this section, first current control based on positive and negative sequence components is investigated. Because zero-sequence voltages of unbalanced voltage dips do not propagate in three-wire systems, or in four-wire system only through secondary side star-ungrounded or delta connected transformers, most case-studies only consider positive and negative sequences. Even for unbalanced systems with zero-sequence voltage, four-leg inverter topologies can eliminate zero-sequence current with appropriate control, and no power introduced by zero-sequence components exist. Nevertheless, to understand the contribution of zero-sequence components to active power control, detailed study is also carried out in this paper.

Positive and negative sequence control

Simplifying assumptions we will use:

- Only positive- and negative-sequence currents are present.
- Only fundamental components exist, the power introduced by harmonics is vanishingly small.
- The amplitude of the positive-sequence voltage is higher than the negative sequence, that is $\|\mathbf{v}^+\| > \|\mathbf{v}^-\|$.

Since no zero-sequence currents are involved, \mathbf{i}_p can be separated into \mathbf{i}_p^+ and \mathbf{i}_p^- , which will be defined in phase with \mathbf{v}^+ and \mathbf{v}^- , respectively, in order to yield active power only. Rewriting (9) and (10) in terms of \mathbf{i}_p^+ and \mathbf{i}_p^- , we obtain

$$p = \underbrace{\mathbf{v}^+ \cdot \mathbf{i}_p^+}_{P^+} + \underbrace{\mathbf{v}^- \cdot \mathbf{i}_p^-}_{P^-} + \underbrace{\mathbf{v}^+ \cdot \mathbf{i}_p^- + \mathbf{v}^- \cdot \mathbf{i}_p^+}_{\tilde{p}_{2\omega}}, \quad (11)$$

$$q = \underbrace{\mathbf{v}_\perp^- \cdot \mathbf{i}_p^+ + \mathbf{v}_\perp^+ \cdot \mathbf{i}_p^-}_{\tilde{q}_{2\omega}}, \quad (12)$$

where P^+ and P^- denote average active power introduced by positive and negative sequences, respectively, and $\tilde{p}_{2\omega}$ and $\tilde{q}_{2\omega}$ are oscillating active and reactive power at twice the grid fundamental frequency.

Because oscillating active power can reflect a variation on the DC-link voltage, and high DC voltage variation may cause over-voltage problems, output distortion, or even control instability, it is desirable to eliminate $\tilde{p}_{2\omega}$. On the other hand, the oscillating reactive power $\tilde{q}_{2\omega}$ also causes power losses and operating current rise, and it therefore is advantageous to mitigate $\tilde{q}_{2\omega}$ as well. A trade-off between $\tilde{p}_{2\omega}$ and $\tilde{q}_{2\omega}$ is not straightforward and depends on practical requirements. In the following, strategies to achieve controllable oscillating active and reactive power are derived from two considerations.

a) Controllable oscillating active power

For given constant active power P , the first two terms of (11) are designed to meet

$$P = \mathbf{v}^+ \cdot \mathbf{i}_p^+ + \mathbf{v}^- \cdot \mathbf{i}_p^-. \quad (13)$$

Since the two terms of $\tilde{p}_{2\omega}$ in (11) are in-phase quantities that add to each other, it is expected that these two terms can compensate each other. By setting intentionally

$$\mathbf{v}^+ \cdot \mathbf{i}_p^- = -k_p \mathbf{v}^- \cdot \mathbf{i}_p^+, \quad 0 \leq k_p \leq 1, \quad (14)$$

after some manipulations, the negative-sequence current \mathbf{i}_p^- is derived from (14) as

$$\mathbf{i}_p^- = \frac{-k_p \mathbf{v}^+ \cdot \mathbf{i}_p^+}{\|\mathbf{v}^+\|^2} \mathbf{v}^-. \quad (15)$$

Substituting (15) into (13), we obtain

$$P \|\mathbf{v}^+\|^2 = (\|\mathbf{v}^+\|^2 - k_p \|\mathbf{v}^-\|^2) (\mathbf{v}^+ \cdot \mathbf{i}_p^+). \quad (16)$$

Then, based on (15) and (16), currents \mathbf{i}_p^+ and \mathbf{i}_p^- can be calculated as

$$\mathbf{i}_p^+ = \frac{P}{\|\mathbf{v}^+\|^2 - k_p \|\mathbf{v}^-\|^2} \mathbf{v}^+, \quad \mathbf{i}_p^- = \frac{-k_p P}{\|\mathbf{v}^+\|^2 - k_p \|\mathbf{v}^-\|^2} \mathbf{v}^-. \quad (17)$$

Finally, the total current reference is the sum of \mathbf{i}_p^+ and \mathbf{i}_p^- , that is

$$\mathbf{i}_p^* = \mathbf{i}_p^+ + \mathbf{i}_p^- = \frac{P}{\|\mathbf{v}^+\|^2 - k_p \|\mathbf{v}^-\|^2} (\mathbf{v}^+ - k_p \mathbf{v}^-), \quad 0 \leq k_p \leq 1. \quad (18)$$

b) Controllable oscillating reactive power

Instead of compensating the oscillating active power in (11), we can similarly shape the oscillating reactive power in (12). For this purpose negative-sequence currents are imposed to meet

$$\mathbf{v}_\perp^+ \cdot \mathbf{i}_p^- = -k_p \mathbf{v}_\perp^- \cdot \mathbf{i}_p^+, \quad 0 \leq k_p \leq 1. \quad (19)$$

By considering equation $\mathbf{v}_\perp^+ \cdot \mathbf{i}_p^- = -\mathbf{v}^+ \cdot \mathbf{i}_{p\perp}^-$, the left side of (19) can be rewritten as

$$\mathbf{v}_\perp^+ \cdot \mathbf{i}_p^- = -\mathbf{v}^+ \cdot \mathbf{i}_{p\perp}^- = -k_p \mathbf{v}_\perp^- \cdot \mathbf{i}_p^+, \quad (20)$$

where $\mathbf{i}_{p\perp}^-$ denotes the orthogonal vector of \mathbf{i}_p^- according to (2). Then, it follows that

$$\mathbf{i}_{p\perp}^- = \frac{k_p \mathbf{v}^+ \cdot \mathbf{i}_p^+}{\|\mathbf{v}^+\|^2} \mathbf{v}_\perp^-. \quad (21)$$

Therefore the negative-sequence current \mathbf{i}_p^- can be calculated by

$$\mathbf{i}_p^- = \frac{k_p \mathbf{v}^+ \cdot \mathbf{i}_p^+}{\|\mathbf{v}^+\|^2} \mathbf{v}^-. \quad (22)$$

Solving (22) and (13), the positive-sequence current and negative-sequence currents are derived as

$$\mathbf{i}_p^+ = \frac{P}{\|\mathbf{v}^+\|^2 + k_p \|\mathbf{v}^-\|^2} \mathbf{v}^+, \quad \mathbf{i}_p^- = \frac{k_p P}{\|\mathbf{v}^+\|^2 + k_p \|\mathbf{v}^-\|^2} \mathbf{v}^-. \quad (23)$$

Again, the total current reference is the sum of \mathbf{i}_p^+ and \mathbf{i}_p^- , that is

$$\mathbf{i}_p^* = \mathbf{i}_p^+ + \mathbf{i}_p^- = \frac{P}{\|\mathbf{v}^+\|^2 + k_p \|\mathbf{v}^-\|^2} (\mathbf{v}^+ + k_p \mathbf{v}^-), \quad 0 \leq k_p \leq 1. \quad (24)$$

c) Combining strategies a) and b)

Simple analysis reveals that (18) and (24) can be combined and represented by

$$\mathbf{i}_p^* = \mathbf{i}_p^+ + \mathbf{i}_p^- = \frac{P}{\|\mathbf{v}^+\|^2 + k_p \|\mathbf{v}^-\|^2} (\mathbf{v}^+ + k_p \mathbf{v}^-), \quad -1 \leq k_p \leq 1. \quad (25)$$

In order to analyze the variation on instantaneous power, we substitute (25) into (11) and (12), and the results are

$$p = P \left[1 + \frac{(1 + k_p) (\mathbf{v}^+ \cdot \mathbf{v}^-)}{\|\mathbf{v}^+\|^2 + k_p \|\mathbf{v}^-\|^2} \right] \quad (26)$$

$$q = P \left[\frac{(1 - k_p) (\mathbf{v}^+ \cdot \mathbf{v}_\perp^-)}{\|\mathbf{v}^+\|^2 + k_p \|\mathbf{v}^-\|^2} \right]. \quad (27)$$

It can be seen that the variant terms of (26) and (27), i.e. oscillating active power and reactive power, are controlled by the coefficient k_p . These two parts of oscillating power are orthogonal and equal in maximum amplitude. Simulation is carried out by sweeping parameter k_p , as shown in Fig. 2. It is illustrated that either oscillating active power or oscillating reactive power can be controlled and even can be eliminated at the two extremes of the k_p curve. This characteristic allows to enhance control flexibility and system optimization. Further discussion will be presented later on.

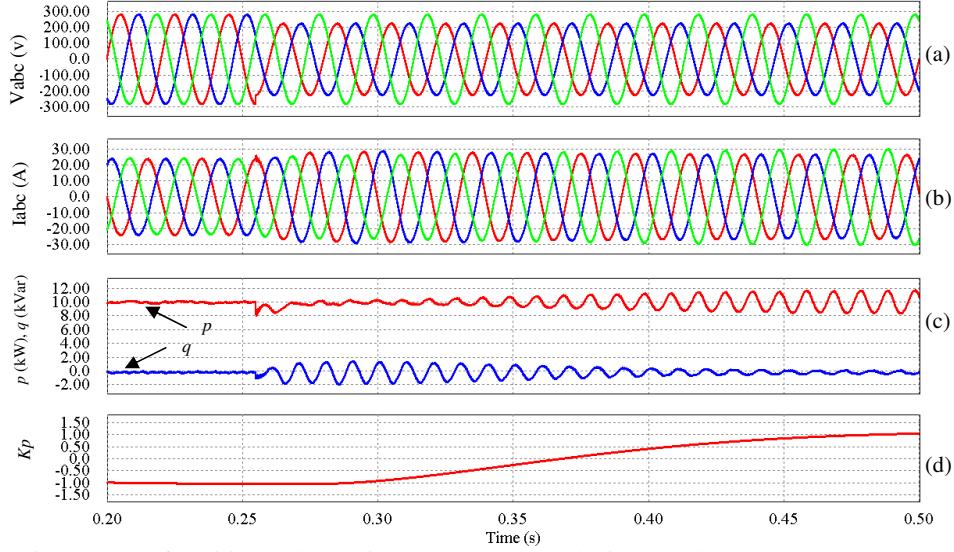


Fig. 2: Simulation results of positive and negative sequence control with $P=10\text{kW}$, $Q=0$, where voltages of phase A and B dip to 80% at $t=0.255\text{s}$, (a) phase voltages, (b) injected currents, (c) instantaneous p , q , and (d) controllable coefficient k_p sweeping from -1 to 1.

Control including zero-sequence currents

It is assumed that zero-sequence components are either not available or eliminated in the above strategy. Although zero-sequence currents are not expected to enter the grid from DG, it is still interesting to investigate the contribution of zero-sequence current when delivering active power. Therefore, the current reference generation of a four-wire DG inverter can become more flexible due to the extra degree of freedom of generating a zero-sequence component. Note that a four-leg inverter topology is required in order to fully control zero-sequence currents.

Active power caused by zero-sequence quantities, named p^0 , can only exist if there are both zero-sequence current \mathbf{i}^0 and voltage \mathbf{v}^0 . Since p^0 only exists in terms of active power, it can only be used to compensate the oscillating active power. Negative-sequence current is utilized to cancel the oscillating reactive power, this has already been derived in the previous section. From (9), we obtain

$$p = \underbrace{\mathbf{v}^+ \cdot \mathbf{i}_p^+}_{P^+} + \underbrace{\mathbf{v}^- \cdot \mathbf{i}_p^-}_{P^-} + \underbrace{\mathbf{v}^+ \cdot \mathbf{i}_p^- + \mathbf{v}^- \cdot \mathbf{i}_p^+}_{\tilde{p}_{2\omega}} + \underbrace{\mathbf{v}^0 \cdot \mathbf{i}_p^0}_{P^0 + \tilde{p}_{2\omega}^0}, \quad (28)$$

where P^0 and $\tilde{p}_{2\omega}^0$ represent the average power and oscillating power produced by the zero-sequence components. Separating (28) into two parts, that is constant power and oscillating power, yields

$$P = \underbrace{\mathbf{v}^+ \cdot \mathbf{i}_p^+}_{P^+} + \underbrace{\mathbf{v}^- \cdot \mathbf{i}_p^-}_{P^-} + P^0 \quad (29)$$

$$\tilde{p} = \underbrace{\mathbf{v}^+ \cdot \mathbf{i}_p^- + \mathbf{v}^- \cdot \mathbf{i}_p^+}_{\tilde{p}_{2\omega}} + \tilde{p}_{2\omega}^0. \quad (30)$$

Substituting (22) into (29) and (30), we obtain

$$\mathbf{i}_p^+ = \frac{P - P^0}{\|\mathbf{v}^+\|^2 + k_p \|\mathbf{v}^-\|^2} \mathbf{v}^+ \quad (31)$$

$$\tilde{p} = \underbrace{(1 + k_p) \mathbf{v}^- \cdot \mathbf{i}_p^+}_{\tilde{p}_{2\omega}} + \tilde{p}_{2\omega}^0. \quad (32)$$

We expect that $\tilde{p}_{2\omega}^0$ can compensate $\tilde{p}_{2\omega}$, hence appropriate zero-sequence currents should meet

$$\tilde{p}_{2\omega}^0 = -\tilde{p}_{2\omega} = -(1 + k_p) \mathbf{v}^- \cdot \mathbf{i}_p^+, \quad (33)$$

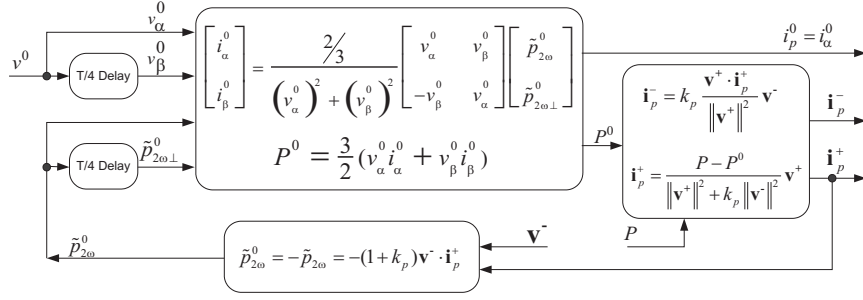


Fig. 3: Structure diagram for generating controllable reference currents based on symmetric sequences.

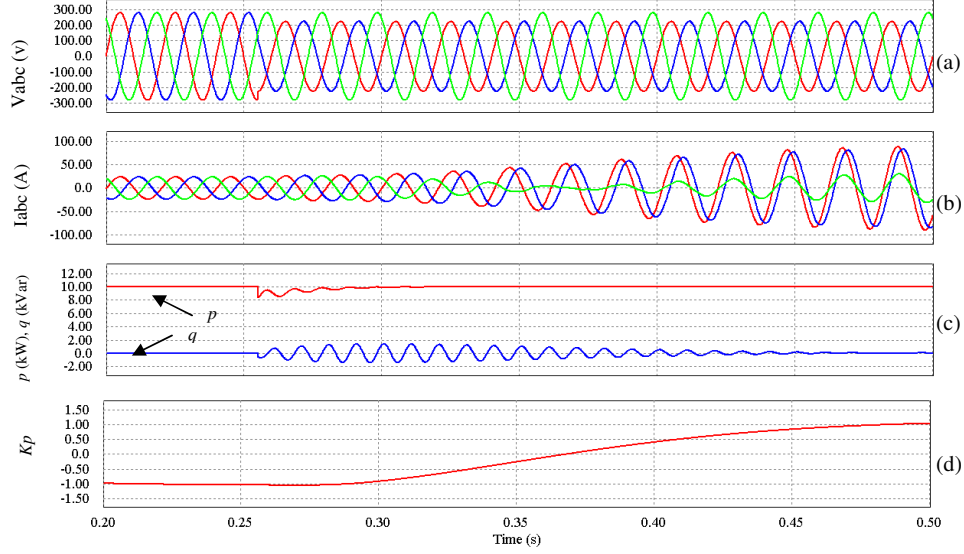


Fig. 4: Simulation results of control including all symmetric sequences with $P=10\text{kW}$, $Q=0$, where voltages of phase A and B dip to 80% at $t=0.255\text{s}$, (a) phase voltages, (b) injected currents, (c) instantaneous p , q , and (d) controllable coefficient k_p sweeping from -1 to 1.

For a certain $\tilde{p}_{2\omega}^0$ given by (33), the corresponding zero-sequence current can be calculated by

$$\begin{bmatrix} i_{\alpha}^0 \\ i_{\beta}^0 \end{bmatrix} = \frac{2/3}{(v_{\alpha}^0)^2 + (v_{\beta}^0)^2} \begin{bmatrix} v_{\alpha}^0 & v_{\beta}^0 \\ -v_{\beta}^0 & v_{\alpha}^0 \end{bmatrix} \begin{bmatrix} \tilde{p}_{2\omega}^0 \\ \tilde{p}_{2\omega\perp}^0 \end{bmatrix}, \quad (34)$$

where $\tilde{p}_{2\omega\perp}^0$ denotes a 90° lagging signal of $\tilde{p}_{2\omega}^0$, v_{α}^0 equals the zero-sequence grid voltage, v_{β}^0 denotes 90° lagging signal of v_{α}^0 , i_{α}^0 represents zero-sequence current and i_{β}^0 the 90° lagging signal of i_{α}^0 (See the derivation in the appendix). Using (31) to (34), current reference generation based on positive, negative, and zero sequences is shown in Fig. 3. Note that the calculation block deriving \mathbf{i}_p^- and \mathbf{i}_p^+ in the diagram actually is the strategy of positive and negative sequence control when P^0 equals zero.

To observe the contribution of zero-sequence currents, numerical simulation was used to generate Fig. 4 under the same grid dip condition as in Fig. 2. As shown in Fig. 4, constant active power is achieved because of the contribution of zero-sequence components. However, when the parameter k_p is getting close to 1, the output currents become severely unbalanced with a large amplitude increase in the phase currents. Because the zero-sequence voltage is much less than the positive-sequence voltage, a large proportion of zero-sequence components is then needed to compensate the oscillating active power introduced by positive and negative sequence currents. Admittedly, the strategy utilizing zero-sequence currents is not practical when the zero-sequence voltage of grid is too small. Unbalanced phase currents would increase sharply, seriously reducing the operation margin of the inverter and causing large unbalanced voltage drop across line impedances. Therefore, the following experiments will only verify the strategy of positive and negative sequence control.

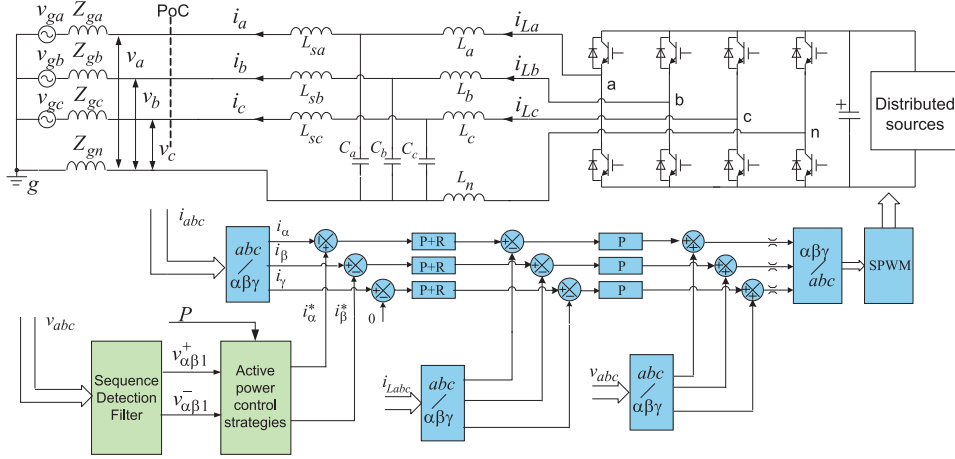


Fig. 5: Circuit diagram and control structure of experimental four-leg inverter system.

Experimental Verification

To verify the strategy of positive and negative sequence control, experiments are carried out on a laboratory prototype which is constructed from a four-leg inverter that is connected to the grid through LCL filters (L_{abc} , L_{sabc} are 2mH, C_{abc} are 5uF, and L_n is 0.67mH), as shown in Fig. 5. By using a four-leg inverter, zero-sequence currents can be eliminated when the grid has zero-sequence voltages. For the cases where the zero-sequence voltage of unbalanced grid dips is isolated by transformers, a three-leg inverter can be applied. A 15KVA three-phase programmable AC power source (SPITZENBERGER+SPIES DM 15000/PAS) is used to emulate the unbalanced utility grid, and the distributed source is implemented by a dc power supply providing a 750V dc bus voltage. The controller is designed on a dSPACE DS1104 setup by using Matlab Simulink.

The proposed controller is realized by a double-loop current controller, which consists of an outer control loop with proportional-resonant (PR) controllers for eliminating the steady-state error of the delivered currents, and an inner inductor current control loop with simple proportional gain to improve stability. In addition, a feed-forward of the grid voltages is used to improve system response to grid voltage disturbances. A detailed design for the PR controller has been presented in [7], it is not duplicated here. The detection of positive and negative sequences is based on a stationary frame filter cell in the $\alpha - \beta$ frame [8]. By shifting the controllable parameter k_p , the system is tested with $P=2500W$ and $Q=0$ when the grid voltage turns to be faulty at $t = 0.03s$ where phase A and B dip to 80%. In order to capture the transient reaction of the system, three situations are tested for comparison. The measured results are shown in Fig. 6. The proposed strategy does give the same results as the simulation in Fig. 2 when k_p equals -1, 0 and 1.

Discussion

It should be emphasized that the proposed current reference generation strategy introduces control flexibility, i.e., the coefficient k_p can be optimally determined based on optimization objectives. Considering the power-electronic converter constraints, a serious problem for the inverters is the second-order ripple on the DC bus, which reflects to the AC side and creates oscillating active power during unbalanced voltage dips. Either for facilitating DC-bus voltage control or for minimizing the DC bus capacitors, it is preferred to decrease k_p to make the ripple as small as possible. However, the maximum deliverable average power has to decrease because unbalanced phase currents reduce the operating margin of inverters. Therefore, for a maximum power-tracking system it is preferable to shift k_p towards zero as long as the variation on dc-link is acceptable. Since power ripples and phase currents can be calculated in real time based on the proposed strategy, k_p can be adaptively changed depending on the process requirements.

On the other hand, the effects of the proposed strategy on the power system side could impose constraints on the control design, especially for large scale DG systems. Oscillating reactive power causes extra power losses in the grid, explaining a preference for k_p close to 1. However, as shown in the results

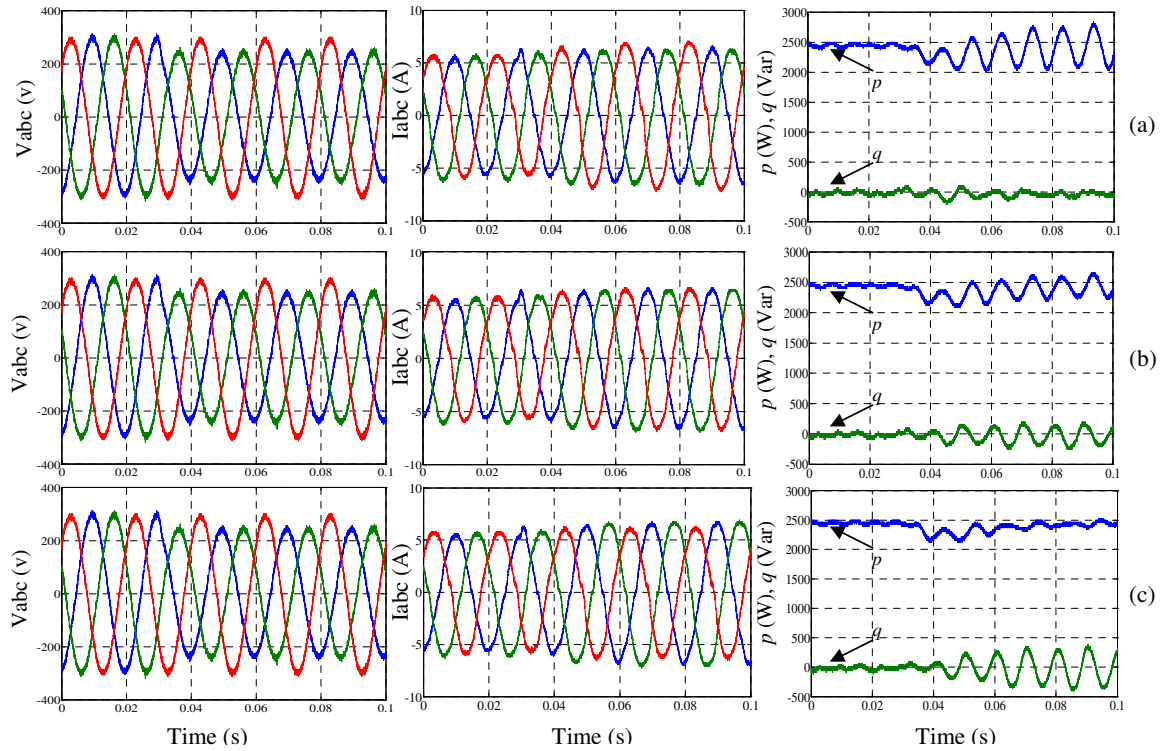


Fig. 6: Experimental results of the proposed control strategy with the adjustable coefficient being set at (a) $k_p = 1$, (b) $k_p = 0$, and (c) $k_p = -1$, where the waveforms from left to right are grid voltages, injected currents, and instantaneous p, q . $P=2500\text{W}$, $Q=0$, voltages of phase A and B dip to 80% at $t=0.03\text{s}$.

of Fig. 2 and Fig. 6, when k_p is getting close to 1, less current is delivered into the phases where grid voltage is relatively high. Consequently, unbalanced voltages are worsened due to voltage rise across grid impedances. On the contrary, when k_p is close to -1, higher current is delivered into the phases where grid voltage is relatively small, thereby compensating the voltage imbalance at the point of connection (PoC) with the grid. Therefore, depending on the practical situation and the requirements from grid codes, the different objectives above can be optimally achieved with the proposed strategy.

The instantaneous power control discussed so far has been treated using the voltage at PoC. Unfortunately, the output inductors of inverters also introduce oscillating power when unbalanced currents flow through them. Hence, part of the active power is supplied by the inverter side from the dc bus when using the proposed strategy. If the oscillating power on account of the output inductors cannot be neglected in case of large and unbalanced currents, the fundamental components of the inverter-bridge output voltages should be used in the above calculations instead of the grid voltages. Then the grid will provide part of the oscillating power due to the inductors.

Conclusion

This paper presents an active power control strategy for distributed generation systems during unbalanced voltage dips. The strategy can facilitate on-line performance optimization of the inverters during voltage dips, i.e., improving grid-fault ride-through capabilities. The proposed strategy for eliminating second-order power ripple by including fundamental zero-sequence components is technically effective. However, it is worth noticing that a serious phase unbalance and a large amplitude increase appear in the current waveforms when using zero-sequence components. Simulations and experiments were carried out and verified the proposed control strategy. Finally, an optimal application of the proposed strategy is further discussed from the perspective of both inverter and grid. Key objectives that depending on practical applications and requirements from grid codes may constrain the choice of the adaptive coefficient in the control strategy are presented.

Appendix

The power introduced by zero-sequence components in a three-phase unbalanced system is similar to that in a single-phase system, always including a constant and an oscillating power. Therefore the following method can also be used for single-phase applications. For the zero-sequence components:

$$i^0 = \sqrt{2}I^0 \cos(\omega t + \theta^0), v^0 = \sqrt{2}V^0 \cos(\omega t + \varphi^0), \quad (\text{A.1})$$

where I^0 and θ^0 are the amplitude and phase angle of the current; V^0 and φ^0 are the amplitude and phase angle of the voltage. The instantaneous power of a three-phase system can be expressed as

$$p^0 = 3v^0 i^0 = \underbrace{3I^0 V^0 \cos(\theta^0 - \varphi^0)}_{P^0} + \underbrace{3I^0 V^0 \cos(2\omega t + \theta^0 + \varphi^0)}_{\tilde{p}_{2\omega}^0}. \quad (\text{A.2})$$

By means of a T/4 delay, two sets of orthogonal signals can be generated, i.e.

$$\begin{aligned} i_{\alpha}^0 &= i^0 = \sqrt{2}I^0 \cos(\omega t + \theta^0), & i_{\beta}^0 &= \sqrt{2}I^0 \sin(\omega t + \theta^0), \\ v_{\alpha}^0 &= v^0 = \sqrt{2}V^0 \cos(\omega t + \varphi^0), & v_{\beta}^0 &= \sqrt{2}V^0 \sin(\omega t + \varphi^0). \end{aligned} \quad (\text{A.3})$$

Therefore, the average power P^0 and oscillating component of p^0 can be represented by

$$\tilde{p}_{2\omega}^0 = \frac{3}{2}(v_{\alpha}^0 i_{\alpha}^0 - v_{\beta}^0 i_{\beta}^0) = 3I^0 V^0 \cos(2\omega t + \theta^0 + \varphi^0) \quad (\text{A.4})$$

$$P^0 = \frac{3}{2}(v_{\alpha}^0 i_{\alpha}^0 + v_{\beta}^0 i_{\beta}^0) = 3I^0 V^0 \cos(\theta^0 - \varphi^0). \quad (\text{A.5})$$

An orthogonal signal of $\tilde{p}_{2\omega}^0$ is also derived, by shifting signals,

$$\tilde{p}_{2\omega\perp}^0 = \frac{3}{2}(v_{\alpha}^0 i_{\beta}^0 + v_{\beta}^0 i_{\alpha}^0) = 3I^0 V^0 \sin(2\omega t + \theta^0 + \varphi^0). \quad (\text{A.6})$$

Rewriting (A.4) and (A.6) in matrix form, we obtain

$$\begin{bmatrix} \tilde{p}_{2\omega}^0 \\ \tilde{p}_{2\omega\perp}^0 \end{bmatrix} = \frac{3}{2} \begin{bmatrix} v_{\alpha}^0 & -v_{\beta}^0 \\ v_{\beta}^0 & v_{\alpha}^0 \end{bmatrix} \begin{bmatrix} i_{\alpha}^0 \\ i_{\beta}^0 \end{bmatrix}. \quad (\text{A.7})$$

The inverse transformation of (A.7) is

$$\begin{bmatrix} i_{\alpha}^0 \\ i_{\beta}^0 \end{bmatrix} = \frac{2/3}{(v_{\alpha}^0)^2 + (v_{\beta}^0)^2} \begin{bmatrix} v_{\alpha}^0 & v_{\beta}^0 \\ -v_{\beta}^0 & v_{\alpha}^0 \end{bmatrix} \begin{bmatrix} \tilde{p}_{2\omega}^0 \\ \tilde{p}_{2\omega\perp}^0 \end{bmatrix}. \quad (\text{A.8})$$

References

- [1] E.ON Netz GmbH: Grid Code for high and extra high voltage, April, 2006. www.eon-netz.com.
- [2] Sannino A., Bollen M., Svensson J.: Voltage tolerance testing of three-phase voltage source converters, IEEE Transactions on Power Delivery, vol. 20, no. 2, pp. 1633-1639, Apr. 2005.
- [3] Chong H., Li R., Bumby J.: Unbalanced-grid-fault ride-through control for a wind turbine inverter, IEEE Transactions on Industrial Applications, vol.44, no. 3, pp. 845-856, May/Jun. 2008.
- [4] Otadui I., Viscarret U., Caballero M., Rufer A., Bacha S.: New optimized PWM VSC control structures and strategies under unbalanced voltage transients, IEEE Transactions on Industrial Electronics, vol. 54, no. 5, pp. 2902-2914, Oct. 2007.
- [5] Akagi H., Watanabe E. H., Aredes M.: Instantaneous power theory and applications to power conditioning, IEEE press, 2007.
- [6] Rodriguez P., Timbus A., Teodorescu R., Liserre M., Blaabjerg F.: Flexible active power control of distributed power generation systems during grid faults, IEEE Transactions on Industrial Electronics, vol. 54, no. 5, pp. 2583-2592, Oct. 2007.
- [7] Zmood D., Holmes D.: Stationary frame current regulation of PWM inverters with zero steady-state error, IEEE Transactions on Power Electronics, vol. 18, no. 3, pp. 814-822, May 2003.
- [8] Wang F., Duarte J., Hendrix M.: High performance stationary frame filters for symmetrical sequences or harmonics separation under a variety of grid conditions, IEEE APEC 2009.